Additional measurements of the microwave properties of some absorbing materials

Robert Chiang

7 August 1994

INTRODUCTION

The planned CESR upgrades involve using superconducting cavities with strongly damped higher order modes(HOM). A layer of microwave absorbing material, ferrite, attached to the inside of the beam tube should provide the desired damping, while avoiding harmful interaction with the beam. In order to choose the right material, we must predict mode damping and beam interaction of the possible materials. These predictions require knowing the microwave properties of each material over a range of frequencies.

Walter Hartung has already measured the μ and ϵ of various possible materials and discussed the theory and results in previous SRF notes 930113/01 and 930322/04. Therefore, this paper will not dwell any more on the theory behind the measurements and calculations, but rather discuss some of the new measurements, as well as improvements in experimental techniques. This paper will first discuss three different aspects of the experimental technique that were tested. Then, it will discuss the results of the new materials measured and provide some interpretation.

EXPERIMENTAL TECHNIQUES

STANDARD PROCEDURE:

In order to clarify the various techniques tested, some of the procedure presented in the previous notes will be summarized. First, samples were made from materials of interest by cutting out cylindrical "beads". A "bead" was then placed in a 7mm coaxial air line such that one face of the sample is at one end of the coaxial line. Good contact between the sample and the coaxial line is important; any air gap will change the capacitance and inductance of the measurements and thereby affect the ϵ and μ values. When measuring compressible material like Teflon, good contact can be ensured by making samples that fit snugly inside the coaxial line. However, since the materials of interest are non-compressible ferrite tiles, another method must be used to achieve good contact. Liquid metal, an alloy of indium and gallium, was applied to surfaces of the "beads" that came in direct contact with the coaxial line before insertion. The liquid metal fills the air gaps between the sample and the coaxial line. To avoid damaging the commercial coaxial lines with liquid metal, a custom-made air line was used.

The S-parameters of the samples were measured for the frequencies between 300KHz and 20GHz using two Hewlett-Packard network analysers, an HP 8753C and an HP 8720A. The frequencies were divided into three segments: 300KHz to 20MHz, 30MHz to 2GHz, and 200MHz to 20GHz. The first two segments were measured using the HP 8753C and the last segment was measured on the HP 8720A. The coaxial line with the sample was connected to the analysers in two different ways. On the 8753C, the air line was connected directly to port 1 and with a high-quality 7mm cable to port 2. On the 8720A, Adams-Russell cables ending in 7mm connectors were used to connect the coaxial line to both ports.

Before attaching the coaxial line and making measurements, the network analysers were calibrated using the standard "full 2-port" calibration procedure with 7mm kits. After connecting the air line, the reference planes were extended to the faces of the sample with previously measured sample and air line lengths. When extending the ports, we first assumed that one face of the sample is at the port 1 end of the air line, then adjusted the extensions according to the mismatch in the S-parameters. If the extensions are correctly set, the reflection coefficients S11 and S22 should match due to symmetry. If the reference planes are offset, there is a phase difference between the coefficients that is proportional to the offset distance and the frequency.

To acquire data, the network analysers were connected to an HP 9816 computer and a BASIC program was written to control the S-parameter measurements. All the measurements were done with an averaging factor of 16. Four S-parameters were measured, including two "forward," S11 & S21, and two "reverse," S22 & S12. The four S-parameters were transferred into the computer and later analyzed using another BASIC program, written to perform the necessary calculations to deduce permeability μ and permittivity ϵ.

TESTING ASPECTS OF THE MEASUREMENT PROCEDURE:

Three aspects of the experimental technique were tested. First, the coaxial line custom-made by our lab for ferrite measurements was compared with the purchased coaxial lines. Second, the two ways of hooking up the material sample, using either two cables or just one cable, were tested. Lastly, four different calibration procedures for the network analysers were compared.

To compare the custom-made coaxial line with the commercial air line, both air lines were used to measure a Teflon sample on the HP 8720A network analyser. A single calibration of the analyser was performed before the measurements. A Teflon sample was inserted into the commercial air line and measured. After the data was acquired into the computer, the Teflon was then inserted into the custom coaxial line and measured again. The data from both measurements were analyzed and the μ and ϵ graphs were compared with the known μ and ϵ values. They were also compared with each other to see if one was noisier than the other. A similar test was also performed on an air sample to verify the results.

The cable hook-up test was performed only on the HP 8720A analyser. A full 2-port calibration was performed with the 2 cable system hook-up. Then a Teflon sample was measured inside a commercial airline. After acquiring the data, the 1 cable system was connected and the same calibration procedure was performed. Without removing the Teflon sample, the commercial airline was attached to the 1 cable hook-up and measurements followed. Again, these two sets of data were analyzed and the μ and ε graphs were compared with each other. To verify the results, a similar test was performed on a ferrite sample (an IB-004 sample) using the custom air line.

Finally, four slightly different calibration procedures were compared to determine whether a certain calibration will provide a more precise measurement. The calibration used through out this test is the full-2-port calibration, which measures reflection, transmission, and isolation in order to correct the S-parameters. The four various tests simply change the number of averages used in various steps of the calibration. The first combination is the calibration procedure that W. Hartung had adapted; the rest are just slight variations from it. The combinations are listed in table 1 below. Calibration for isolation was completely skipped in two of the cases; past experience has shown that better measurements result from either a lot of averaging for isolation, or no isolation at all. The calibration comparison was performed on both network analysers, covering all 3 frequency segments. The four calibrations were all done and saved in registers before starting the measurements. An IB-004 sample was used for this test. The sample was inserted, with liquid metal applied, into the custom coaxial line, and then hooked up to one of the network analysers. Without removing the sample or the coaxial line, the four calibrations were recalled in order and measurements were taken. Then a similar process was performed on the other network analyzer. Permeability and permittivity graphs for each combination were compared.

Combination #	# Averages for reflection and transmission calibration	# Averages for isolation calibration
1	1	32
2	1	Skip (0)
3	16	32
4	16	Skip (0)

Table 1: Four calibration combinations for network analysers

The calibration procedure that produced the least noise, combination # 3 (see the next section), was used for further ferrite measurements.

RESULTS/DISCUSSION

RESULTS FROM THE TECHNIQUE TESTS:

The results from the three experimental technique tests will be presented first. The first test, the coaxial line comparison, shows that the custom-made coaxial air line is as good as the commercial air lines. Figure 1 shows the μ and ε of a 0.491in long Teflon sample measured with custom and commercial air lines. Both measurements are fairly accurate, having values close to the known microwave properties. The real part of ε is about twice ε_0, and the real part of μ is the same as μ_0. The imaginary parts of both μ and ε are about zero. Both the custom and the commercial coaxial line measurements are fairly noise free, except for the expected large spikes at integer multiples of λ/2. An air sample was also measured to verify the coaxial line test. The results are not shown here since they lead to a similar conclusion; ferrite measurements made with the custom-made coaxial line will be as precise as with a commercial line.

Results from the second test, the cable hook-up comparison, indicate that neither hook-up has an advantage over the other. Figure 2 shows the μ and ε of a 0.971in long Teflon sample measured with the one cable and the two cable setups. Both setups produced fairly accurate results; neither appeared noisier than the other. An IB-004 sample was also measured to verify the hook-up test. The results from the IB-004 measurements are not included in this paper, again because they lead to the same conclusion that both setups are equally precise. Since both setups were acceptable, we decided to adopt the single cable hook-up on the HP 8720A, just to be consistent with the hook-up on the HP 8753C analyser.

Unlike the coaxial line and the hook-up, the calibration procedure did influence the precision of the measurements. The results show small but discernible differences between the four calibration procedures. The third calibration combination from table 1 produced the most precise results. Figures 3,4,5 and 6 show the results from the four calibration procedures. The material measured was a .250in long IB-004 sample. The figures show that the real parts of ε and μ are not very sensitive to the calibration procedures. The real part of ε in figures 5 and 6, where 16 averages were used for reflection and transmission calibration, was perhaps slightly less noisy than in figures 3 and 4 at very high frequencies. However, the real part of μ showed almost no variation between the four cases. The imaginary parts of ε and μ, perhaps more sensitive to calibration because their values are much smaller, are the graphs that truly indicate the superiority of calibration combination #3. The imaginary ε graphs are all very noisy, but the ones in figures 5 and 6 are clearly better at low frequencies. Not only were the graphs in figures 5 and 6 less noisy, but the forward and reverse values also match better. The imaginary μ graphs are probably the best indication that calibration #3 produces the most precise measurements. At low frequencies, the μ graphs in figures 5 and 6 are less noisy than the ones in figures 3 and 4, with figure 5

showing the best match between forward and reverse waves. Since figure 5 corresponds to the third calibration combination, with 16 averages for reflection and transmission, and 32 averages for isolation, this calibration procedure was adopted for further measurements.

In addition to the formal tests mentioned above, another aspect of the measurement was tested informally. Two ways have been used polish the faces of the ferrite samples for measurements. One is to cut the samples to it's proper length with a small circular saw in the Clark technical lab and use a hand grinder to remove any small chips. Another way is to let the machine shop grind the samples to it's proper length. We have wondered whether one way produced better measurements than the other. Through several measurement comparisons, we were able to conclude that neither way had an advantage over the other.

NEW FERRITE MEASUREMENTS:

After verifying our measurement technique, several new ferrites were measured, including some CN-20 samples, a LEAD ferrite, four IB-004 samples that underwent various treatments, and four lots from the TT2-111 series. The results of these measurements are shown in the following pages. The μ and ϵ of all the materials measured appeared to be highly frequency dependent.

Three CN-20 samples with different lengths were measured. Their μ and ϵ results don't seem too different from some of the TT2-111 series ferrites currently used in HOM load tests. Figure 7 shows all three results together for comparison. The imaginary ϵ graph is too noisy for comparison, but the other three graphs in figure 7 show fairly good reproducibility between the three samples. The real μ graph shows almost perfect match between the three samples. However, there are slight differences between the samples in the imaginary μ and real ϵ graphs. At low frequencies, the longest sample (10.3mm) seems to deviate from the other two. Instead of dropping straight down in these graphs, the values of the longest sample seem more reasonable and far less noisy than the other two. This further supports Walter's assertion, given in SRF notes 930113/01 and 930322/04, that we need to avoid having sample lengths which are much less than the wavelength in the material. (i.e. avoid $d<<\lambda$).

Figure 8 shows the measurement results for a ferrite received from the Laboratoire D'electronique et D'Automatique Dauphinois (LEAD). Only one measurement was done on this LEAD ferrite; there was only one sample available to us and it cracked after the first measurement. Since the results could not be verified, they need to be interpreted with some reserve. However, they are probably not too far off since the values are fairly close to the previous ferrite measurements, such as some of the TT2-111 series values. The one questionable graph is the imaginary μ graph. In all the other ferrites measured, the imaginary μ graph shows a distinct peak.

The imaginary μ of the LEAD, however, appears to decrease monotonically as a function of frequency. This could be a real phenomenon, but it needs to be verified with more measurements.

Four IB-004 ferrite samples were received from TDK, each having undergone various treatments, as described in table 2. Figure 9 shows the μ and ϵ of all four samples. All four graphs in figure 9 indicate that the treatments produce significant variations in the microwave properties of IB-004. According to the graphs, the treatment that produced the least amount of change was the simple heating in vacuum. The μ graphs indicate no change at all; the ϵ graphs only show a slight increase relative to the standard. The HIPping and the hot-press processes, however, clearly produced dramatic changes. Both processes shifted the real and imaginary μ curves down almost across the entire frequency range. Comparing only the peak values in the μ graphs, the vacuum hot press process lowers both the real and imaginary μ by almost a factor of 2. The powder HIPping process lowers the μ by almost a factor of 5. Both these processes appear to have the opposite effect on the real and imaginary ϵ of the ferrite. They raised the ϵ of the IB-004 by significant amounts, with the vacuum hot press processes elevating it slightly more. The effects of all these treatments are probably real since the measurements were repeated twice, with similar results.

Treatment	Code Name
None	Standard
Heated in vacuum @ 1050°C for 20 minutes	Heated
Vacuum hot-pressed @ 1000°C for 2 hours pressure used=300 kg/cm^2	Vac Hot Press
First powder HIPped @ 850°C for 2 hours pressure used=1000 kg/cm^2	1st Powder

Table 2: Four IB-004 samples with different treatments

Lastly, four lots of TT2-111 series ferrites were measured. Table 3 shows selected information provided by Trans-Tech on the four ferrites. The measured μ and ϵ of all four ferrites are shown in figure 10. All four lots of TT2-111 appear to have similar μ, both the real and imaginary parts. However, the ϵ values vary greatly between the lots. The real ϵ graph illustrates the significantly larger values of the TT2-111RC ferrite, or lot # 78263. The imaginary ϵ graph shows clear variations between all four ferrites. This is consistent with the notion that imaginary ϵ is due primarily to the DC resistivity. Comparing the imaginary ϵ graph with table 3, the inverse relationship between DC resistivity and imaginary ϵ can be clearly seen. Measurements of all four ferrite samples were repeated and similar results were obtained.

Lot #	Designation	DC Resistivity (Ω cm)
78263	TT2-111RC	784
75074	TT2-111U	5900
82199	TT2-111RF	34400
74837	TT2-111CA	44900

Table 3: Four lots of TT2-111 series ferrite with different resistivities

To further understand how the ferrites would behave as part of an HOM load, the four TT2-111 series ferrites were subjected to some of the treatments that an HOM load would undergo. After each treatment, the microwave properties of the ferrites were measured to see if the treatments affected the ferrites' μ and ε. Table 4 shows the treatments performed on the ferrites. Each of the figures 11-14 corresponds to one of the four ferrites. Each figure has plots from three sets of data, corresponding to the three treatments in table 4. The three data sets are of the exact same ferrite; the ferrites were measured, treated, than remeasured. The "normal" data sets in all four figures is the same as the ones in figure 10; they are just replotted for comparison. The results for frequencies below 200MHz in these figures should not be taken too seriously, as the network analyser 8753C started behaving sporadically during the time of these measurements, most likely due to the wear and tear on the calibration kits. However, the results should not be completely ignored either, since they do provide a general picture about the effects of the treatments. I will point out some of the more questionable measurements so that the data will be useful.

Treatments	Code Name
None	Normal
1. Fired at 900°C in air	900 deg. in air
2. Fired at 250°C in nitrogen (performed on ferrites that were already subjected to #1)	250 deg. in nitrogen

Table 4: The treatments performed on each of the four TT2-111 series ferrites

The "normal" data sets were taken before the sporadic behavior started on the network analysers and should therefore be fairly accurate. However, any deviations from the "normal" in the other two data sets need to be questioned. The real and imaginary μ graphs in all the figures were studied first. Figure 11 shows that neither treatment had any effect on TT2-111RC. Figures 12-14, however, show some differences in the imaginary μ at lower frequencies. I believe that these difference should be ignored, because only the second treatment, the 250°C firing in nitrogen, show these differences. After the first treatment, μ and ε measurements were performed

three times, with only the first measurement shown in the figures. The first two measurements produced similar results, but the third measurement showed the strange behavior at lower frequencies seen in the "250 deg. in nitrogen" data. This indicates that the differences in μ that appears in the second treatment data is more likely due to the network analysers than the treatment. The ε graphs were examined next. I believe that these data are free from any network analyser errors, since the differences between the data sets were introduced by the first treatment. However, the small differences in ε at lower frequencies might be due to the slight chips on the samples. The firing and the repeated measurements had caused tiny pieces to come off the face of some samples. This could certainly distort the measurements by introducing unavoidable air pockets and analyser reference plane errors. The differences in ε are small enough in any case for us to conclude that the firing processes have little, in any, effect on the microwave properties of the TT2-111 ferrites. This conclusion is supported by the IB-004 results discussed above, which also show that just heating the ferrites does not affect their μ and ε much.

CONCLUSION

The coaxial transmission line technique of measuring μ and ε was improved with the new calibration procedures. The liquid metal technique, when applied correctly, continues to give relatively reproducible results. Most of the new measurements discussed in this paper are fairly trustworthy, with the exception of the most recent measurements performed after the network analyser's sporadic behavior. Some of the new μ and ε values discussed in this paper are currently being used in running simulations to predict the behavior of the ferrites in the HOM load high-power test. The simulations should help us understand the power absorption abilities of the ferrites and perhaps save some time later in the CESR upgrade effort.

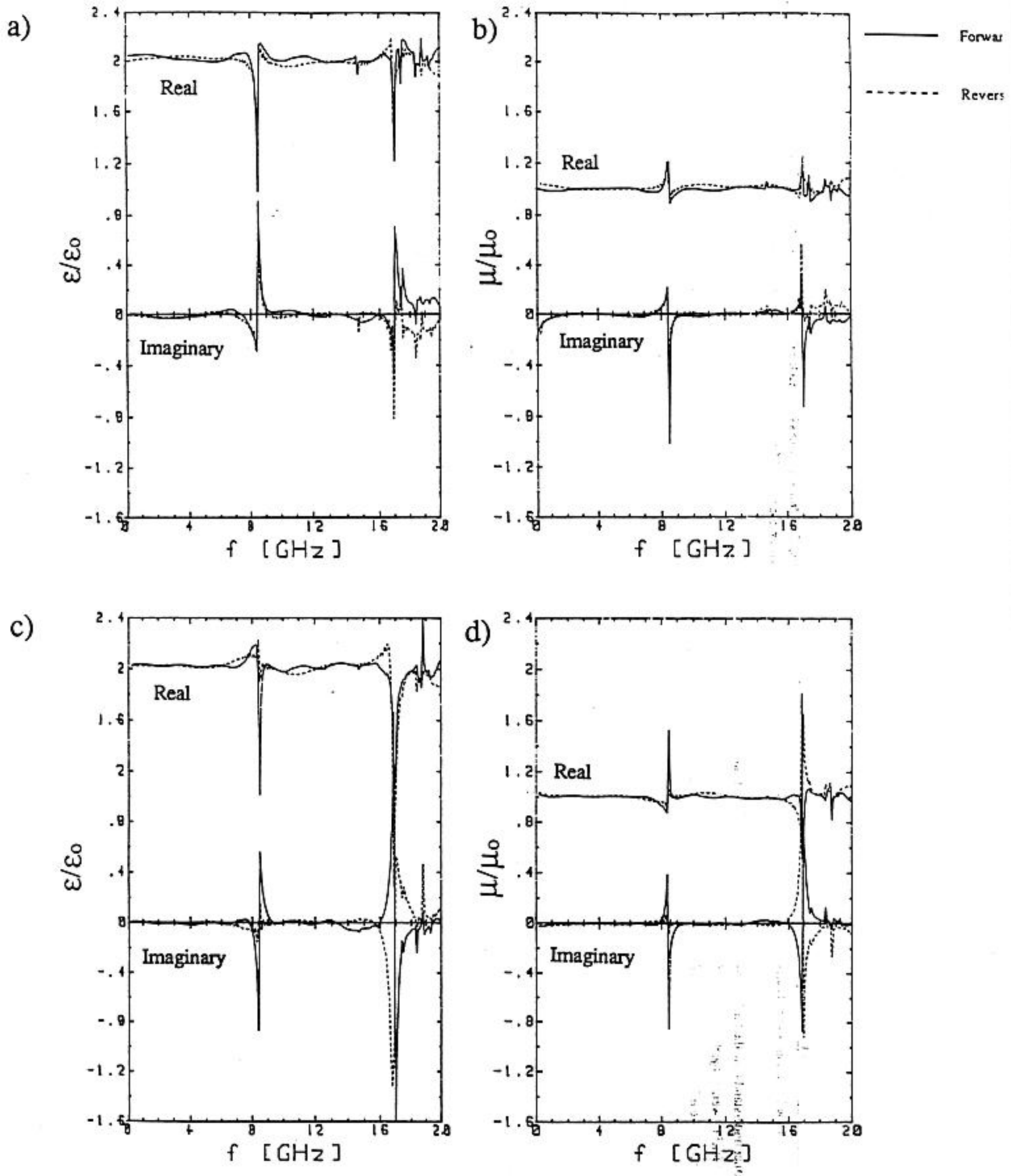

Figure 1: Measured ε and μ of Teflon as a function of frequency. Graphs a) and b) show the measurements using a commercial coaxial line. Graphs c) and d) show the measurements using the custom-made coaxial line.

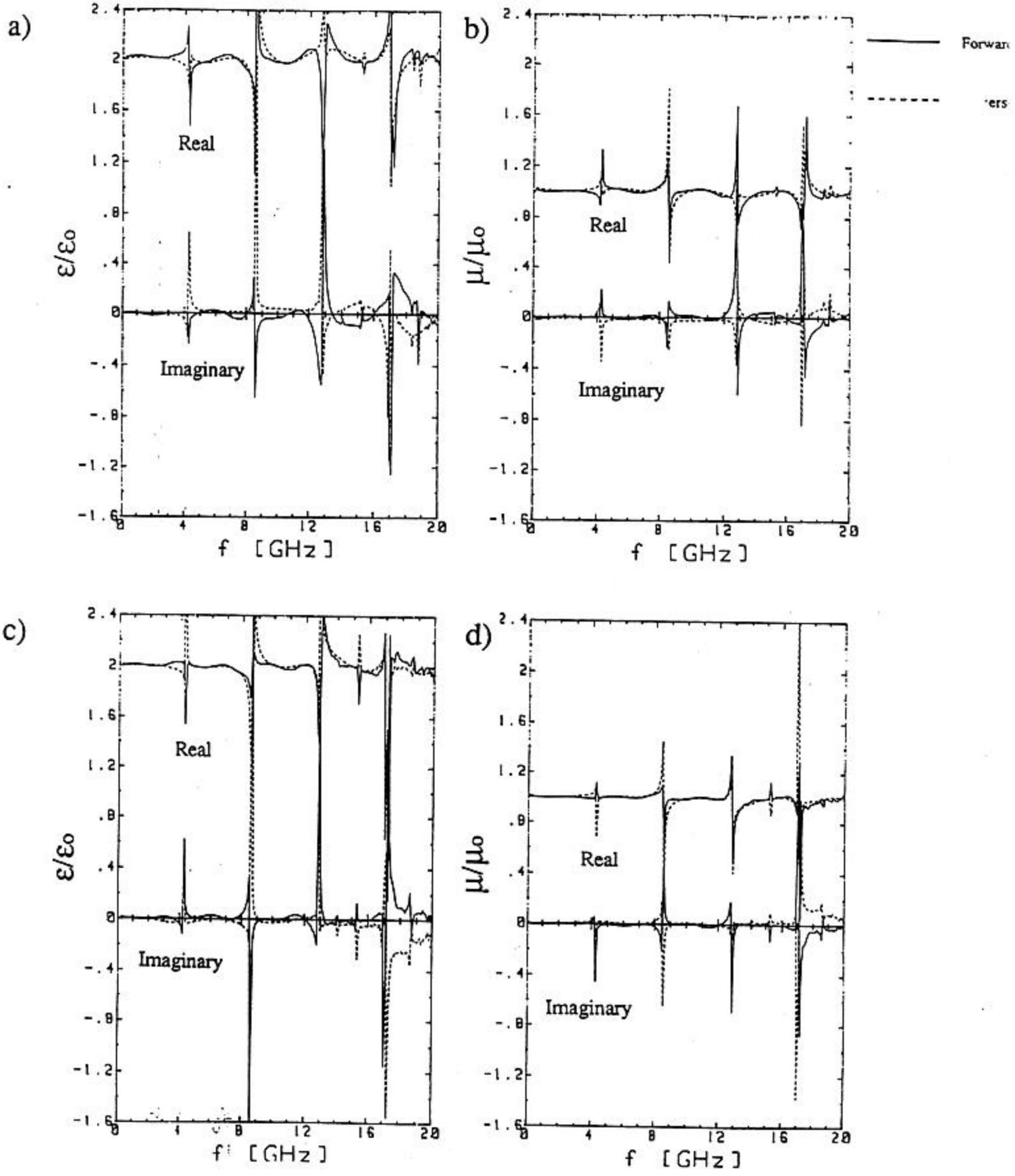

Figure 2: Measured ε and μ for Teflon as a function of frequency. Graphs a) and b) show the measurements using the 1 cable hook-up. Graphs c) and d) show the measurements using the 2 cable hook-up.

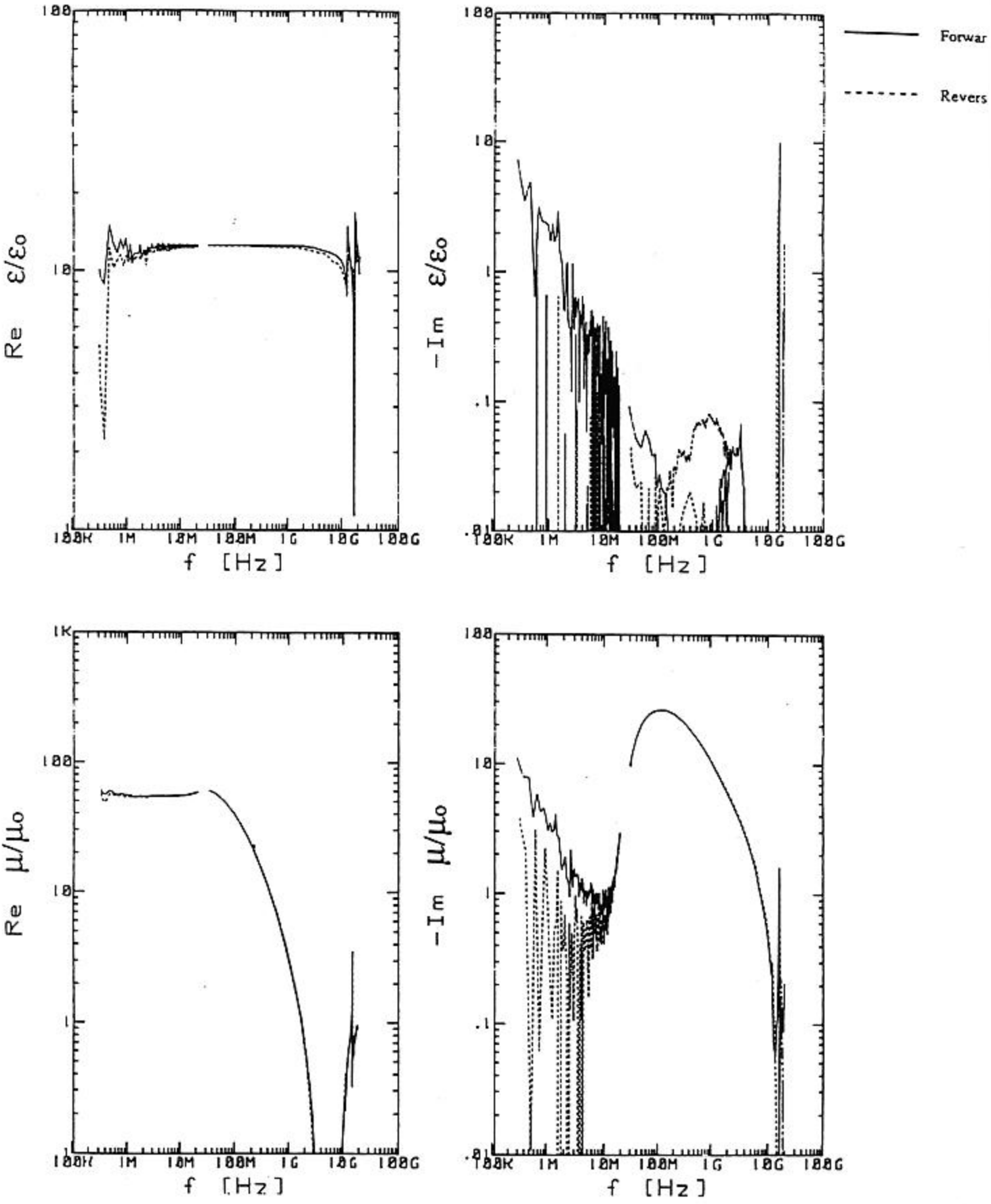

Figure 3: The measured ε and μ of IB-004 as a function of frequency. Calibration procedure #1 from table 1 was used.

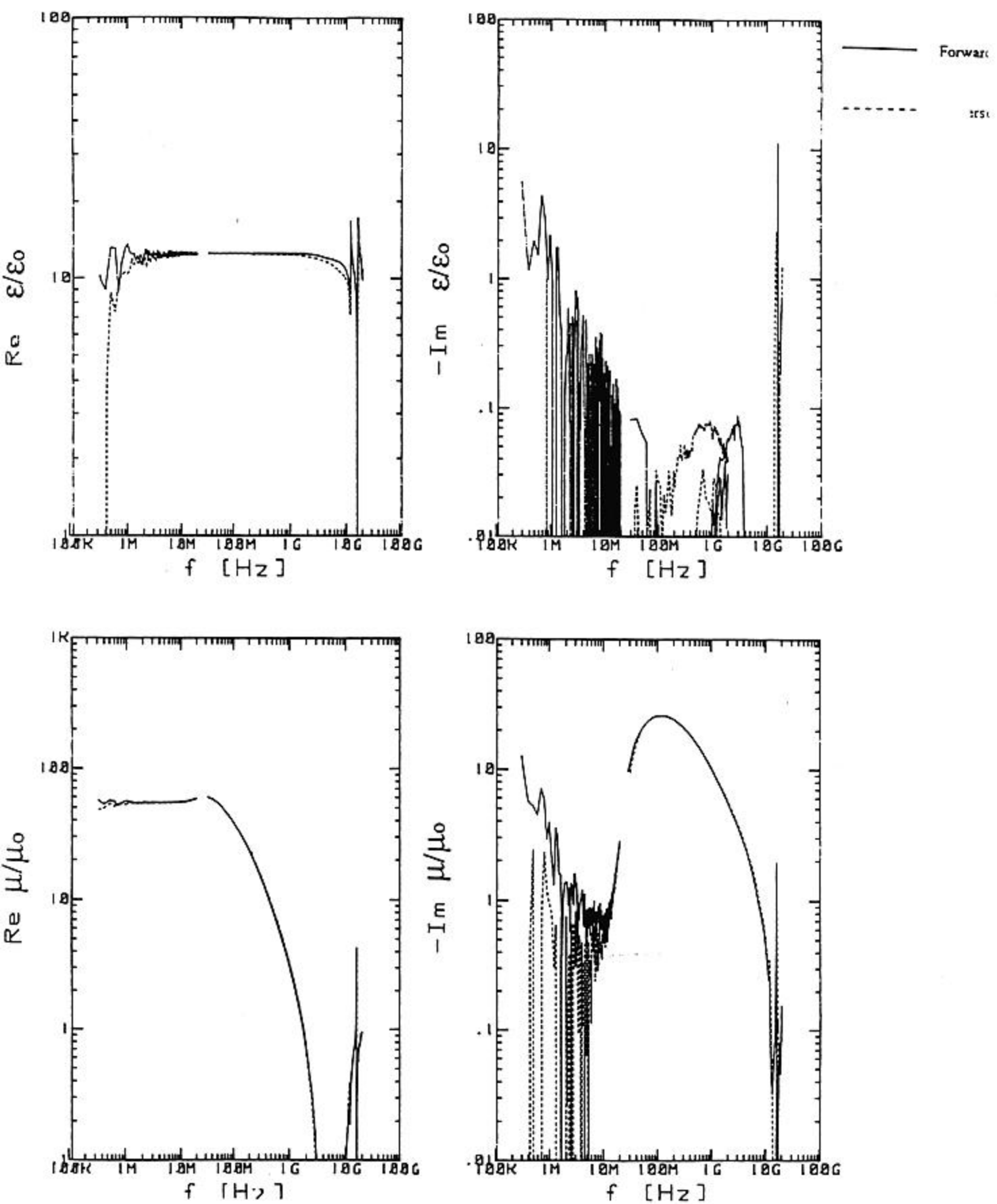

Figure 4: The measured ε and μ of IB-004 as a function of frequency. Calibration procedure #2 from table 1 was used.

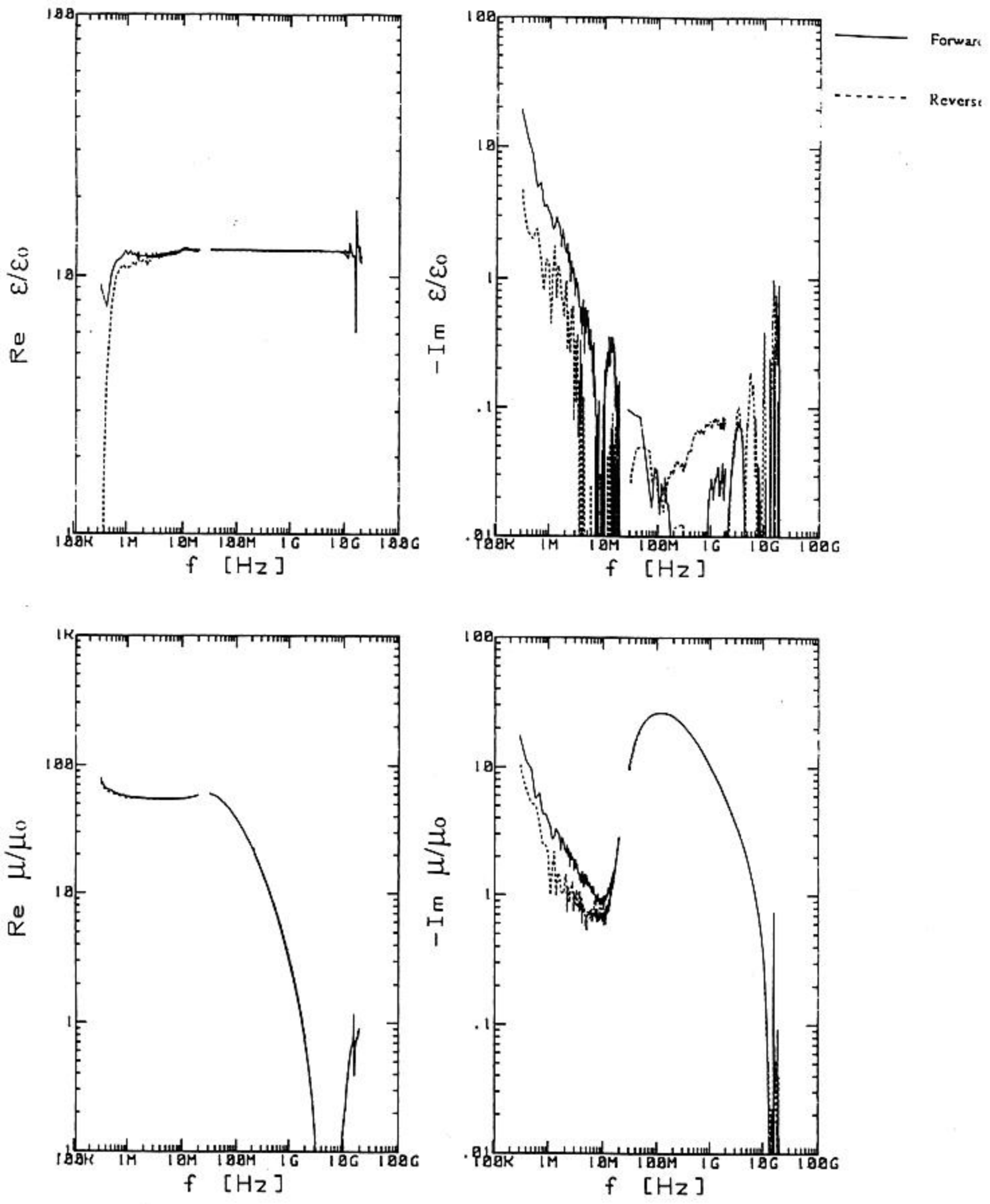

Figure 5: The measured ε and μ of IB-004 as a function of frequency. Calibration procedure #3 from table 1 was used.

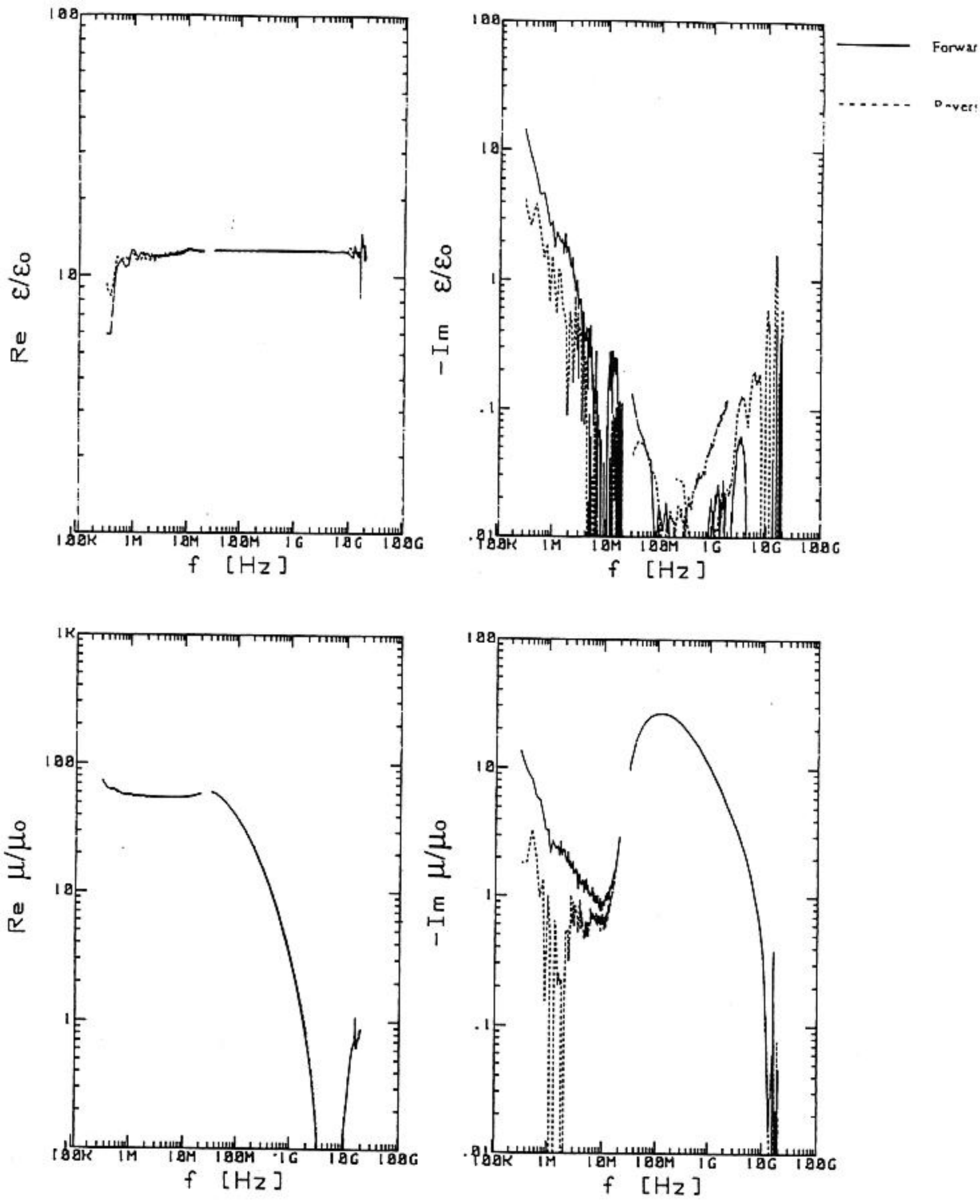

Figure 6: The measured ε and μ of IB-004 as a function of frequency. Calibration procedure #4 from table 1 was used.

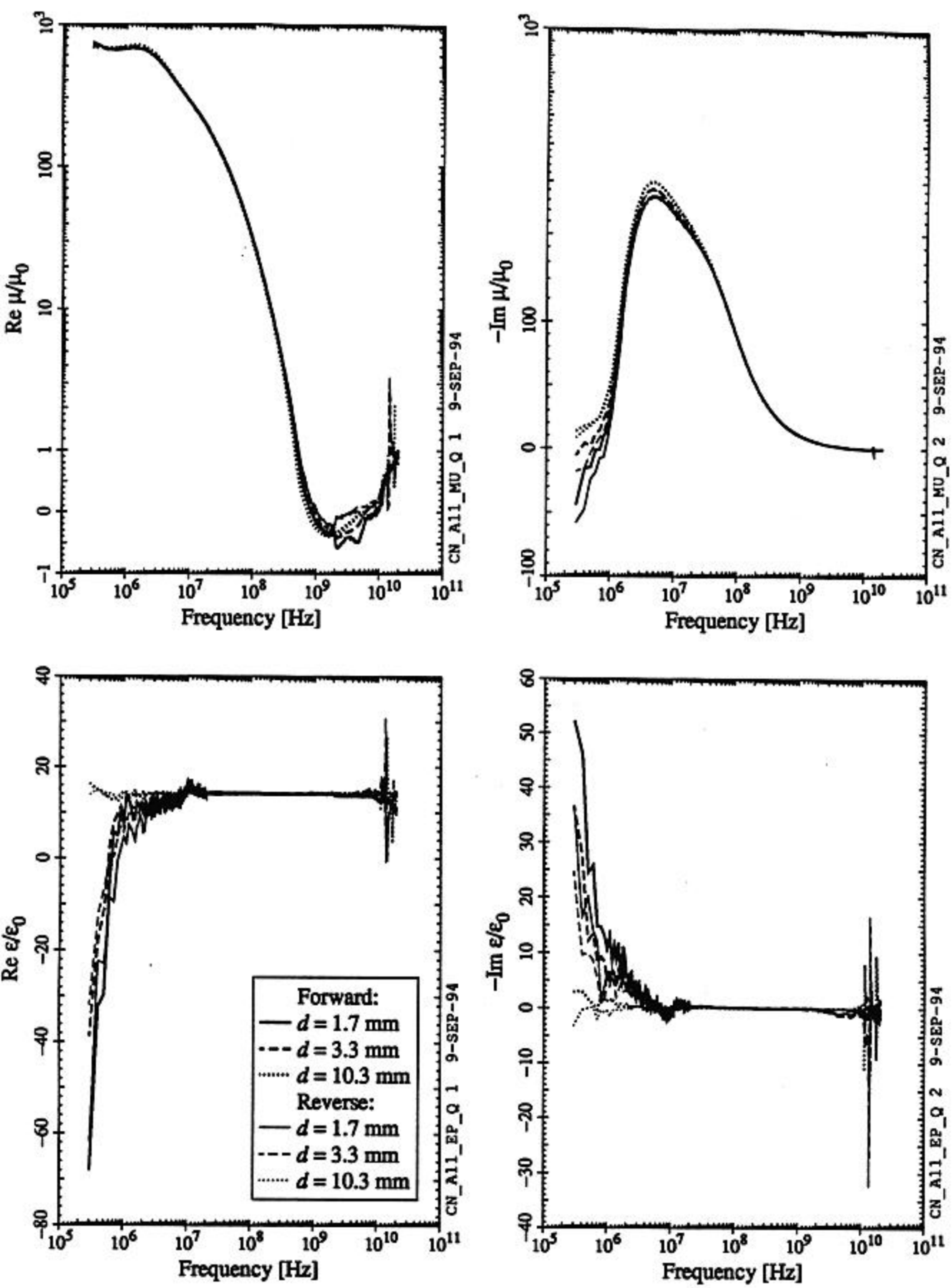

Figure 7: Measured μ and ε of three different lengths of CN-20 samples

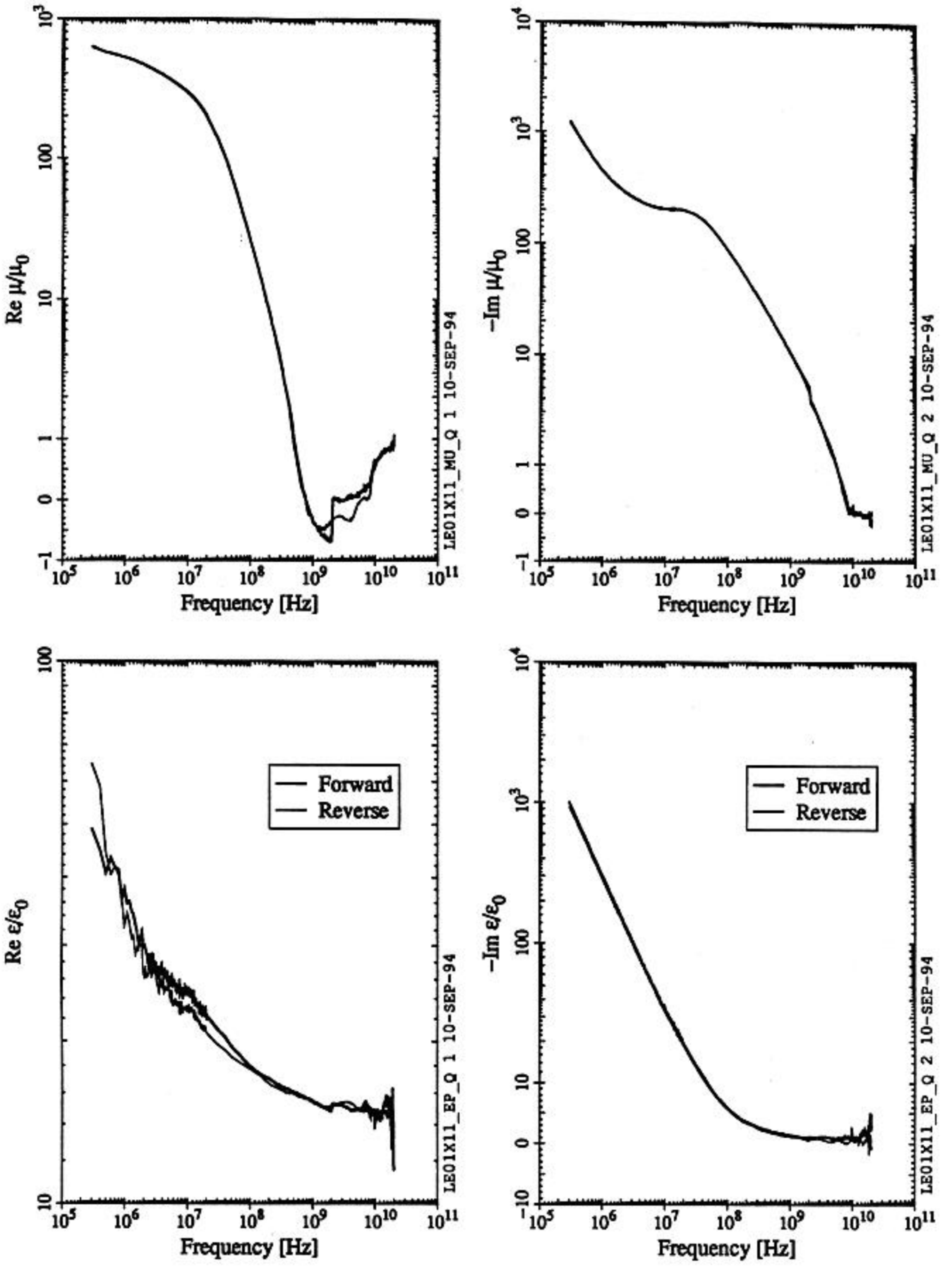

Figure 8: Measured μ and ε of a L.E.A.D. sample

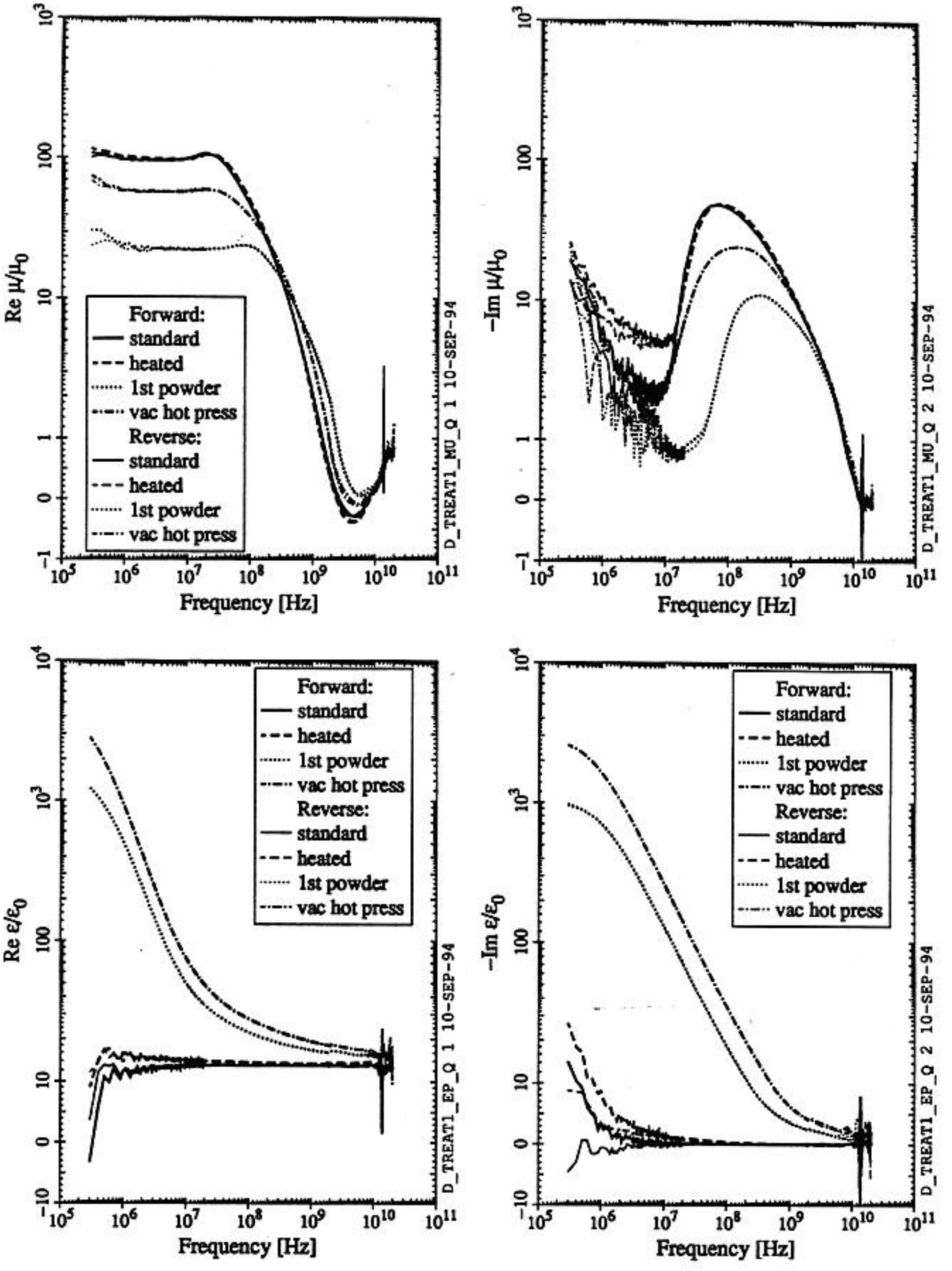

Figure 9: Measured μ and ε of four IB-004 samples from TDK that have undergone various treatments (see table 2)

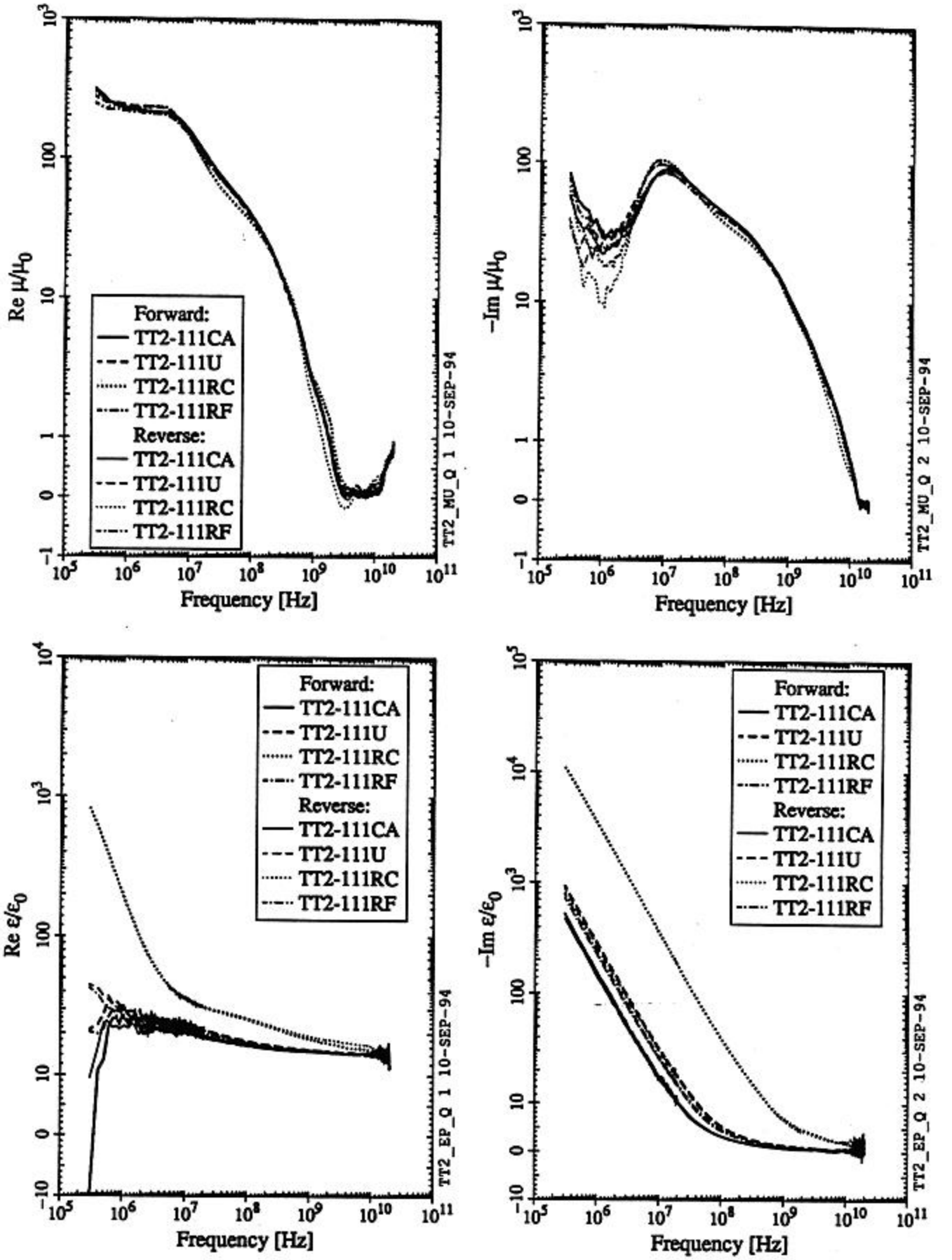

Figure 10: Measured μ and ε of four different lots of TT2-111 series ferrites

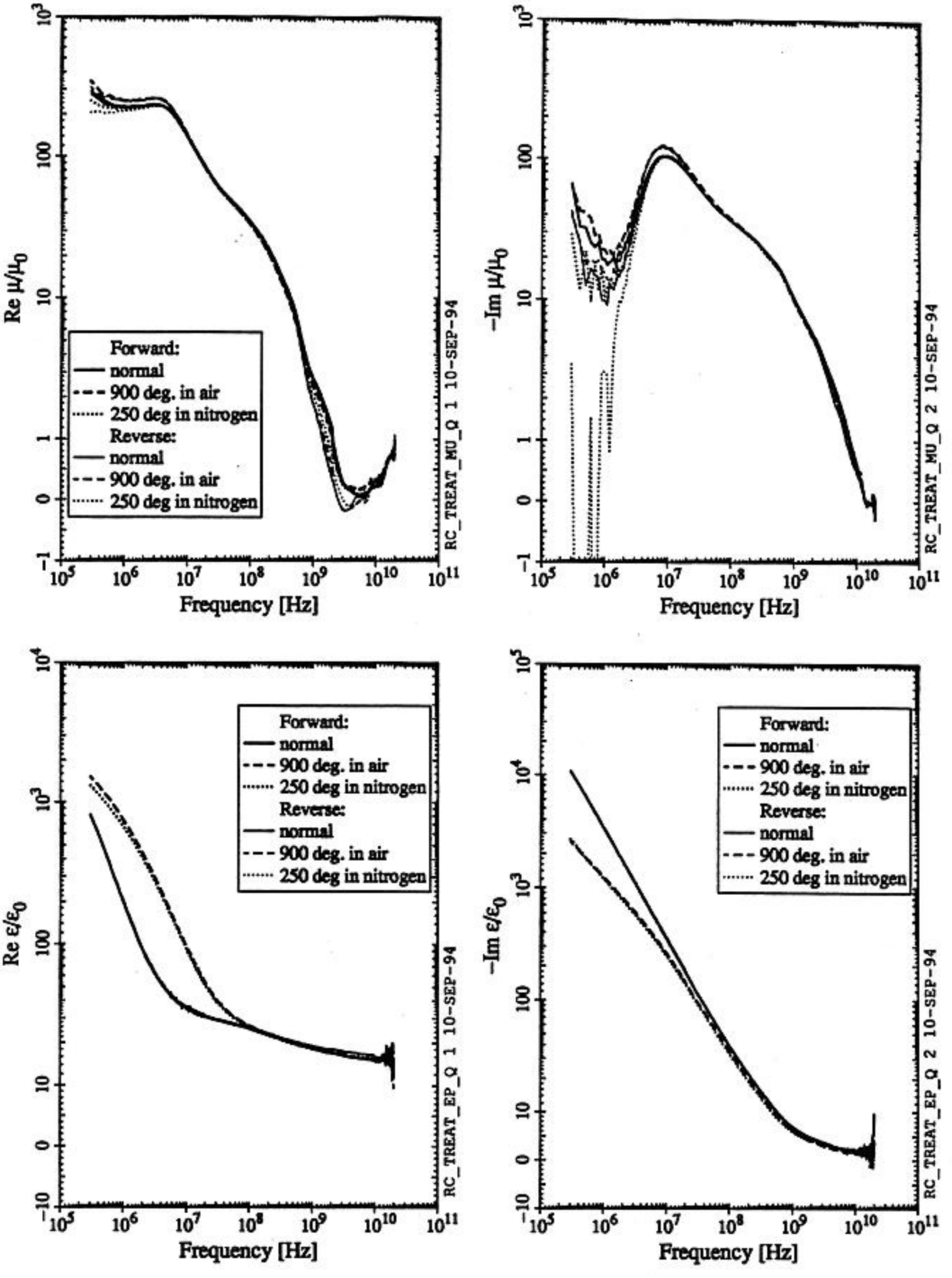

Figure 11: Measured μ and ε of TT2-111RC, illustrating the effect of the various firing processes (see table 4)

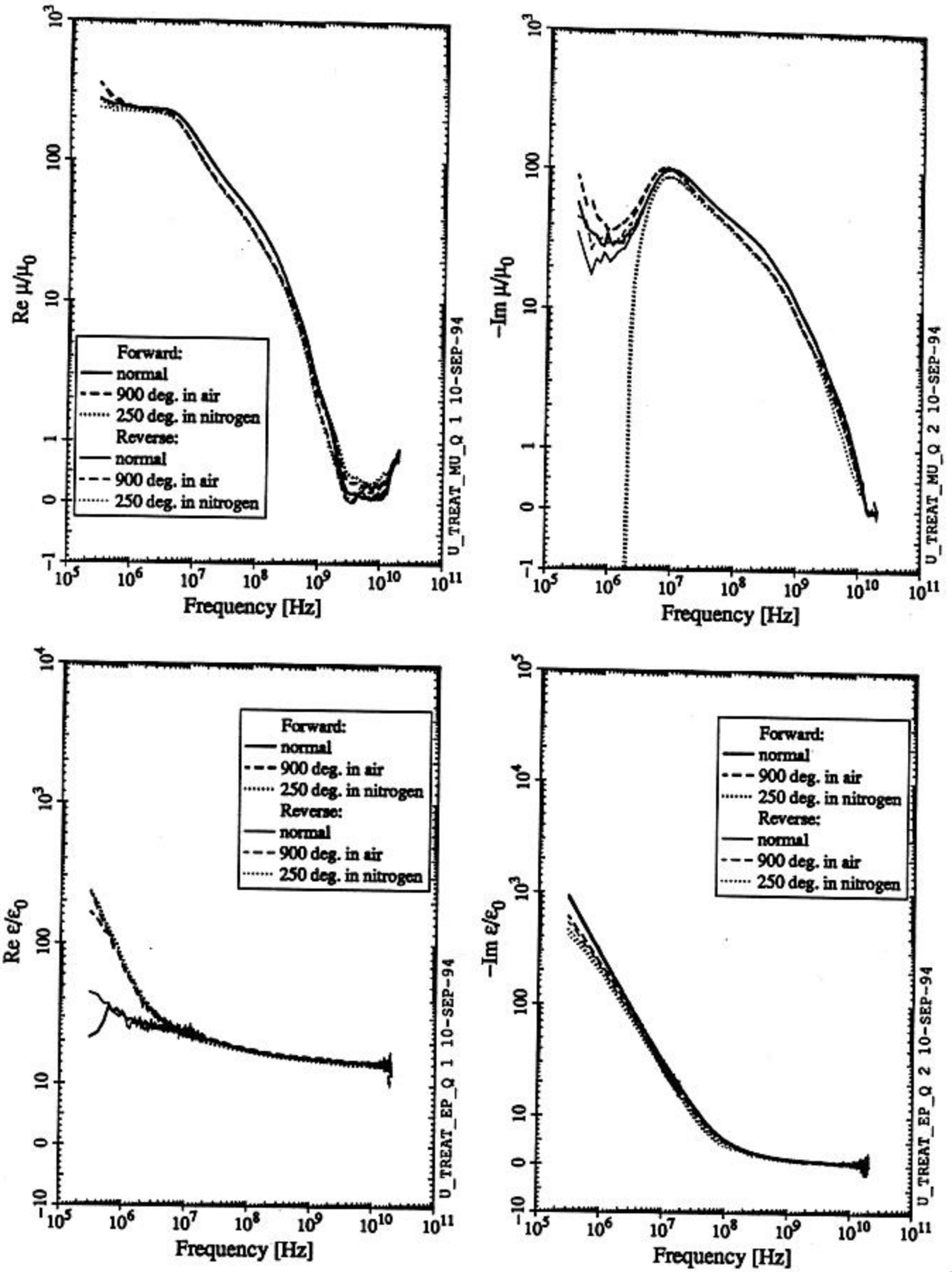

Figure 12: Measured μ and ε of TT2-111U, illustrating the effect of the various firing processes (see table 4)

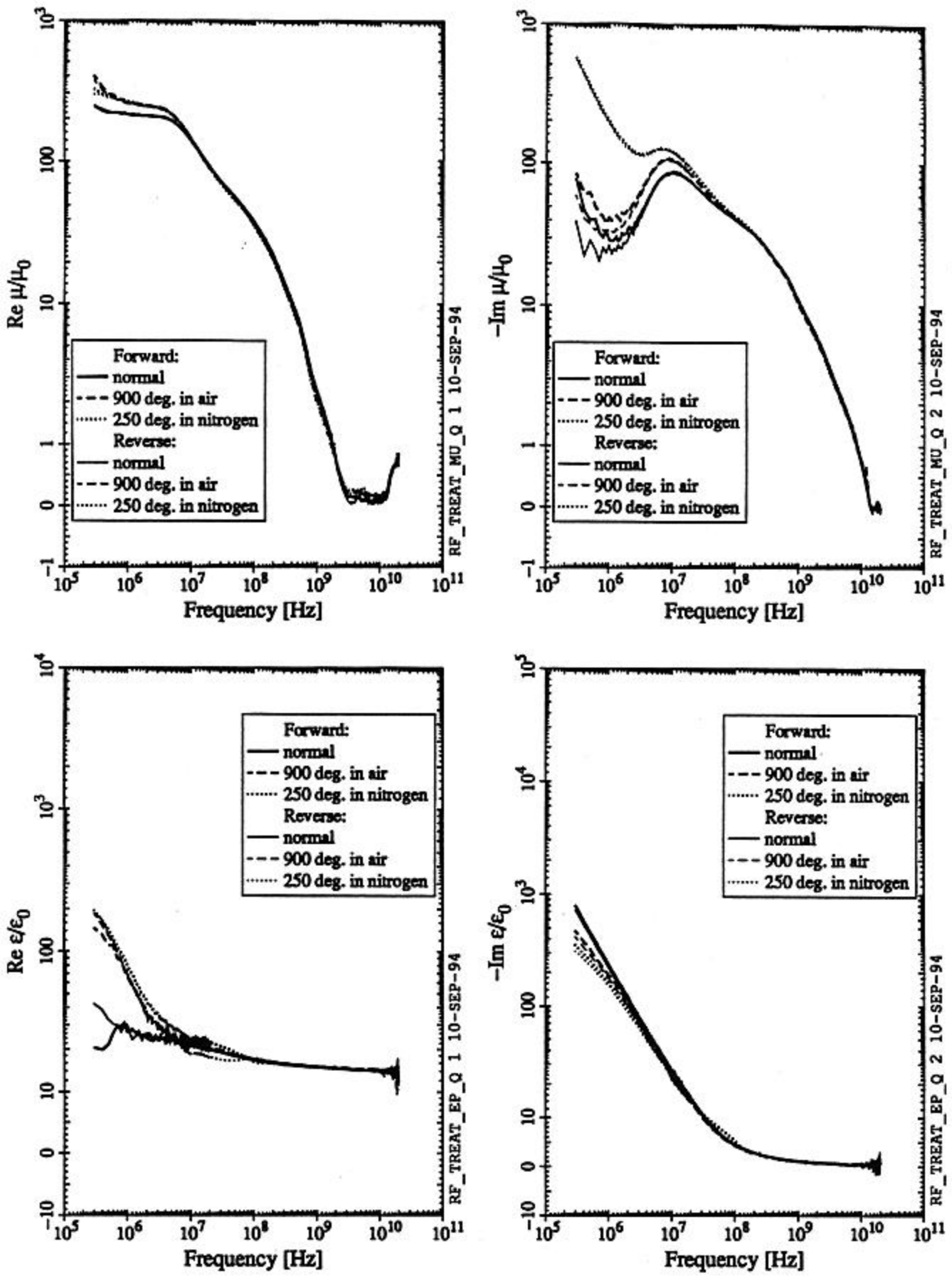

Figure 13: Measured μ and ε of TT2-111RF, illustrating the effect of the various firing processes (see table 4)

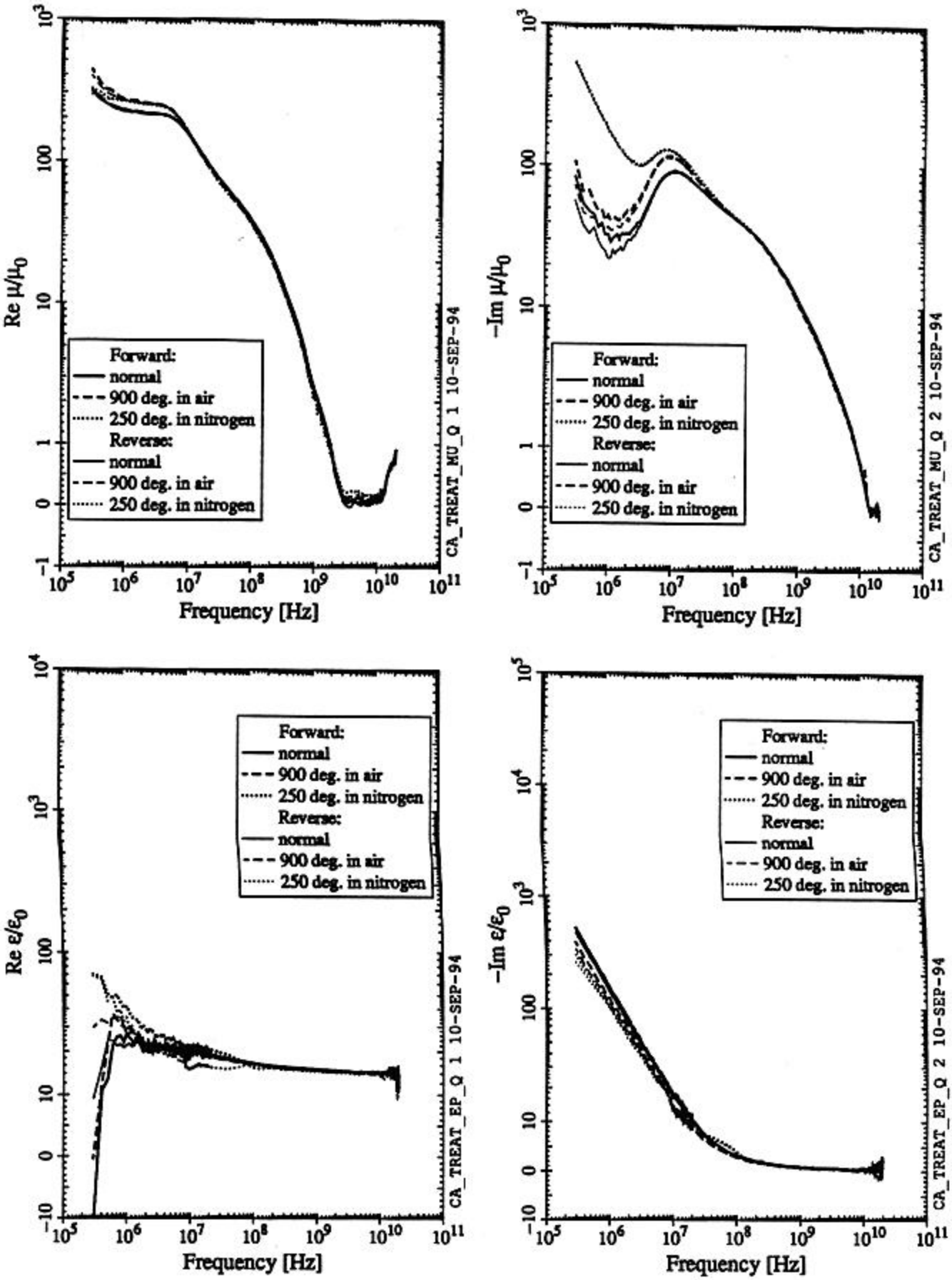

Figure 14: Measured μ and ε of TT2-111CA, illustrating the effect of the various firing processes (see table 4)